Cardiac Blood-Pool Scintigraphy in Rats and Hamsters: Comparison of Five Radiopharmaceuticals and Three Pinhole Collimator Apertures

Pierluigi Pieri, Alan J. Fischman, Marsood Ahmad, Richard H. Moore, Ronald J. Callahan, and H. William Strauss

Division of Nuclear Medicine of the Department of Radiology, Massachusetts General Hospital, and Harvard Medical School, Boston, Massachusetts

Preclinical evaluation of cardiac drugs may require evaluation of cardiac function in intact animals. To optimize the quality of radionuclide measurements of ventricular function in small animals, a comparison was made of gated blood-pool scans recorded with five blood-pool radiopharmaceuticals (^{99m}Tc-labeled human polyclonal IgG, ^{99m}Tc-human serum albumin labeled by two methods, and red blood cells radiolabeled with ^{99m}Tc via in vivo and in vitro methods) in rats and three pinhole apertures in hamsters. The quality of the radiopharmaceuticals was evaluated by comparing count density ratios (LV/BACKGROUND and LV/LIVER) and ejection fractions recorded with each agent. The edge definition of the left ventricle and count rate performance of the 1-, 2-, and 3-mm apertures was evaluated in hamsters. In general, the images obtained with the radiolabeled cells were superior to those obtained with the labeled proteins and no significant differences between the protein preparations were detected. Left ventricular ejection fractions calculated with all five radiopharmaceuticals were not significantly different. The best quality images were obtained with the 1-mm pinhole collimator. Ejection fraction and acquisition time were inversely related to aperture size. A good compromise between resolution and sensitivity was obtained with the 2-mm pinhole collimator.

J Nucl Med 1991; 32:851–855

In the course of evaluating new drugs or therapeutic procedures, it is frequently necessary to perform serial measurements of ventricular function in small laboratory animals. While gated blood-pool scintigraphy is an accurate and widely used method for the serial measurement of ejection fraction (EF) and wall motion abnormalities in man (*1,2*), there are few references describing the use of this technique to evaluate ventricular function in small animals (*3*).

Received Aug. 13, 1990; revision accepted Oct. 6, 1990.

For reprints contact: H. William Strauss MD, Division of Nuclear Medicine, Massachusetts General Hospital, 55 Fruit St., Boston, MA 02114.

To obtain high quality blood-pool images, particularly when repeated studies are performed, it is essential that the radiopharmaceutical remains in the intravascular space. In addition, it is important to choose a collimator that provides an acceptable compromise between resolution and sensitivity.

Radiopharmaceuticals that have been used for blood-pool imaging include: ^{99m}Tc-labeled red blood cells (RBCs) produced by in vitro (*4–6*), in vivo (*7*), modified in vivo (*8*), and whole blood in vitro (*9*) techniques as well as ^{99m}Tc-labeled human serum albumin (HSA) (*10–13*). Several investigators have compared the imaging properties of these agents in humans (*14–19*). In general, it appears that the in vitro and modified in vivo labeling techniques produce the highest quality images and are the most widely used blood-pool radiopharmaceuticals.

RBC radiolabeling techniques are relatively cumbersome to use in small animals. In vitro radiolabeling requires the use of a donor animal for harvesting cells. In vivo radiolabeling requires two i.v. injections. This represents a technical problem in hamsters in whom the very short tail cannot be used for i.v. injection and thus a different approach is necessary. With both methods, cell radiolabeling efficiency is not always predictable and may be influenced by many factors (*16,20–21*). Technetium-99m-labeled HSA has the advantage of ease of preparation and a single injection, but may present problems related to leakage of this radiopharmaceutical into the extravascular space (*10–11,13,14*). Several studies have reported that images recorded with this agent are inferior to those obtained with radiolabeled RBCs (*14–15*).

If a larger protein could be easily radiolabeled with ^{99m}Tc, it might be possible to develop a single injection radiopharmaceutical that has better intravascular retention than HSA. Recently, in the course of studying the infection imaging properties of ^{99m}Tc-labeled IgG (radiolabeled via the nicotinyl hydrazine derivative) (*22*), we observed that blood-pool structures are extremely well defined in early images.

This study was undertaken to compare the image quality of gated blood-pool images recorded with ^{99m}Tc-labeled RBCs to those obtained with ^{99m}Tc-labeled albumin and IgG in rats and hamsters. As we began our investigation, we realized that a potentially confounding variable was physical resolution due to pinhole aperture size. As a result, a parallel study was performed with one radiopharmaceutical to determine the effect of pinhole aperture on image quality.

METHODS

Radiopharmaceuticals

In Vivo Radiolabeled RBCs. For in vivo labeling of RBCs, 70 μg of stannous chloride from a standard pyrophosphate kit were injected intravenously, followed 15 min later by injection of 15 mCi of [^{99m}Tc]pertechnetate.

In Vitro Radiolabeled RBCs. For in vitro labeling, RBCs were obtained from a donor rat which was injected with stannous chloride from a pyrophosphate kit 15 min prior to sacrifice. The cells were washed with saline before adding [^{99m}Tc]pertechnetate. The cells were incubated for 20 min at room temperature and washed twice with saline to remove unbound pertechnetate.

Technetium-99m-Labeled HSA (I) (Stannous Reduction). Technetium-99m-labeled HSA was prepared with a standard kit (Medi-Physics, Paramus, NJ). Radiochemical purity was determined using ITLC-SG chromatographic strips (German Laboratories, Ann Arbor, MI) with normal saline as the solvent.

Technetium-99m-Labeled IgG and ^{99m}Tc-HSA (II). The nicotinyl hydrazine derivatives of IgG and HSA were prepared as previously described (*22*). The modified IgG and HSA were radiolabeled with ^{99m}Tc by reaction with ^{99m}Tc-glucoheptonate that was freshly prepared with a standard kit (Dupont, N. Billerica, MA) (*22*). Radiochemical purity was determined using ITLC-SG chromatographic strips with normal saline as the solvent.

Comparison of Radiopharmaceuticals for Gated Blood-Pool Imaging in Rats

Fifteen millicuries of ^{99m}Tc-labeled radiopharmaceutical were administered to male Sprague-Dawley rats weighing 250–300 g. The rats were anesthetized with pentobarbital (40–50 mg/kg, i.v.) and imaged approximately 1 cm from the pinhole collimator (3-mm insert) of a large field of view gamma camera interfaced to a dedicated computer (Technicare model 438/Technicare model 560, Solon, OH). This configuration resulted in visualization of only the chest of the rat (approximately 12× magnification). Imaging was performed using the projection that provided the best separation between the ventricles (typically a 10–15° LAO). ECG electrodes were attached to the right front limb and the two hind limbs with 22-gauge needles for gating. Thirty-two images were acquired in frame mode using a 64 × 64 matrix. The acquisition was stopped when the count density of the brightest pixel over the heart reached 256. All imaging was performed within 1 hr of injection. Five to eight rats were evaluated with each agent.

Effect of Pinhole Aperture on Cardiac Blood-Pool Imaging in Hamsters

Three aperture sizes were tested in this study. Apertures of 1 mm and 2 mm were fabricated as lead insert disks designed to fit into the standard pinhole collimator holder of the gamma camera.

TABLE 1
Physical Characteristics of Pinhole Collimators

Pinhole diameter	Area relative to 3 mm	Op. range (cm)	Mag. range (x)	FOV (cm)
3 mm	1.00	1.2–37	1.35– 48	0.87–27
2 mm	0.44	0.8–25	2.0 – 63	0.58–18.5
1 mm	0.11	0.4–12.5	4.0 –125	0.30– 9.3

Op. Range (cm) = useful operating range; Mag. range (x) = useful magnification range; and FOV = field of view at magnification end points.

The 3-mm pinhole was supplied by the manufacturer. The physical characteristics of these collimators are shown in Table 1.

Six male Syrian hamsters aged two months and weighing 80–100 g were studied. After anesthesia with ketamine (100 mg/kg, i.m.), 12 mCi of ^{99m}Tc-HSA were administered intravenously through the dorsal vein of the penis. Images were recorded in the LAO 30° projection with the pinhole collimators positioned in contact with the animals chest. The animals were imaged sequentially with the 3-, 2-, and 1-mm apertures. All other aspects of the imaging protocol were identical to that described above. With the 2-mm pinhole collimator, we also studied 11 Syrian hamsters of the myopathic strain Bio TO (8-mo-old) and 9 age-matched controls (Bio Breeders Inc., Watertown, MA).

Data Analysis

Three regions of interest were constructed as follows: left ventricle (LV), paracardiac background adjacent to the left ventricle (BKG), and liver (Fig. 1). Using the same regions of interest for all the diastolic images, count densities were obtained for each radiopharmaceutical. The density ratios, LV/BKG and LV/LIVER, were determined. To calculate ejection fraction of the left ventricle (LVEF), the images were smoothed, lung background (counts/pixel in a region adjacent to the left ventricle) was subtracted, and regions of interest were drawn over the left ventricle. Total counts in the left ventricular regions of interest were determined for each frame of the collection and the LVEF (ED-ES/ED) was calculated. In each study, the EF was calculated independently by two experienced observers.

Statistical Analysis

The results were evaluated by analysis of variance followed by Duncan's new multiple range test. All results are expressed as mean ± s.e.m.

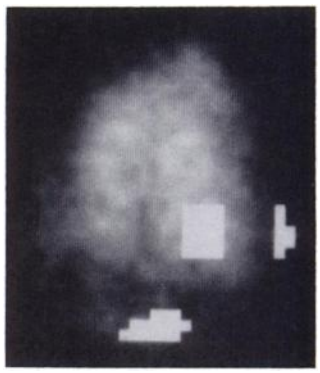

FIGURE 1. Gated blood-pool image of the thorax of a rat indicating the ROIs used to calculate count density ratios and EF, left ventricular blood pool, paracardiac background, and liver.

RESULTS

The radiochemical purity of the in vitro labeled red blood cells was greater than 95%. The radiochemical purity of the radiolabeled proteins was greater than 90%.

Qualitative evaluation of the images showed sufficiently clear separation of the ventricles to permit definite identification of the LV borders with all five radiopharmaceuticals within one hour of injection, however, there was greater lung and liver background with the radiolabeled proteins. Representative images are shown in Figure 2.

Analysis of variance demonstrated that the LV/BKG count density ratio for in vitro radiolabeled RBCs was significantly greater than for ^{99m}Tc-HSA (II) ($p < 0.05$) and the LV/LIVER ratio for in vivo and in vitro radiolabeled RBCs was significantly greater than for the radiolabeled proteins ($p < 0.05$). Ejection fractions measured with in vitro radiolabeled RBCs, IgG, and HSA (I) were similar to each other and slightly higher compared to in vivo RBCs and HSA (II), but no statistically significant differences were detected (Table 2).

In 2-mo-old normal Syrian hamsters, LVEF calculated from images acquired with 1-, 2-, and 3-mm pinhole collimators and the time necessary to reach the same count density are shown in Table 3. The EFs were 60.4 ± 3 (3 mm), 68.7 ± 3 (2 mm), and 73.3 ± 2 (1 mm). The EF measured with the 1-mm pinhole was significantly higher than with the 3-mm pinhole ($p < 0.01$). Images obtained with the different collimators are shown in Figure 3. While it was possible to separate the ventricles with the 3-mm pinhole, the 1- and 2-mm pinholes offered better definition of cardiac structures and great vessels. The highest quality images were obtained with the 1-mm pinhole, but a much longer time was necessary to collect the same number of counts per pixel. A good compromise between resolution and sensitivity was obtained with the 2-mm pinhole (good definition of the cardiac chambers and great vessels with 8 min of data acquisition).

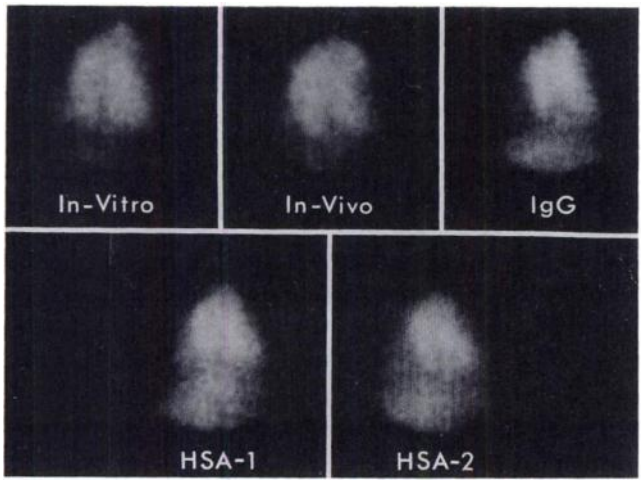

FIGURE 2. End-diastolic images of gated blood-pool studies recorded with five different radiopharmaceuticals: in vitro ^{99m}Tc-RBCs; in vivo ^{99m}Tc-RBCs; ^{99m}Tc-IgG; ^{99m}Tc-HSA (I); and ^{99m}Tc-HSA (II). Note the higher liver activity with Tc-IgG and Tc-HSA.

TABLE 2
Counts Density Ratios and Ejection Fractions in Rats Imaged with Five Radiopharmaceuticals

Method	N	Count density ratio		Ejection fraction (%)
		LV/BKG	LV/Liver	
In vitro RBCs	5	3.10 ± 0.22*	2.32 ± 0.10†	77.6 ± 3.4
In vivo RBCs	6	2.69 ± 0.21	1.89 ± 0.14†	71.2 ± 4.8
IgG	8	2.49 ± 0.19	1.36 ± 0.10	78.2 ± 2.7
HSA (II)	8	2.35 ± 0.22	1.49 ± 0.08	73.5 ± 1.3
HSA (I)	8	2.55 ± 0.18	1.38 ± 0.07	77.1 ± 1.9

* $p < 0.05$ compared to HSA (II).
† $p < 0.05$ compared to the radiolabeled proteins.

When studied with the 2-mm pinhole collimator, the EF of cardiomyopathic Syrian hamsters was significantly lower than age-matched controls (17.3 ± 2.2 versus 58.2 ± 3.9, $p < 0.001$). Representative images are shown in Figure 4.

DISCUSSION

In many experimental protocols with small laboratory animals, serial measurements of LVEF and regional wall motion are important to follow changes in cardiac function. For example, in studies of dilated cardiomyopathy using myopathic strains of Syrian hamsters (*23–24*), it may be important to document the stages of the disease in individual animals to determine the impact of a therapeutic intervention. To follow ventricular function under these circumstances, it is important to obtain good definition of the cardiac chambers and great vessels to draw accurate regions of interest. For this purpose, it is important to choose an optimal radiopharmaceutical and imaging system.

In previous studies, RBCs radiolabeled with ^{99m}Tc by the in vitro, in vivo, and modified in vivo methods have been compared to ^{99m}Tc-labeled HSA for gated blood-pool imaging in humans (*14–19*). The in vitro technique yields the highest quality images, however, the labeling process is relatively complicated and time consuming. In addition, the blood handling that is required is a potential health

TABLE 3
Effect of Pinhole Aperture on Ejection Fraction in Hamsters (n = 6)

Pinhole size (mm)	Ejection fraction (%)	Time (min)*
3	60.4 ± 3	5
2	68.7 ± 3	8
1	73.3 ± 2†	20

* Time to record images of the same count density.
† $p < 0.01$ compared to 3-mm pinhole.

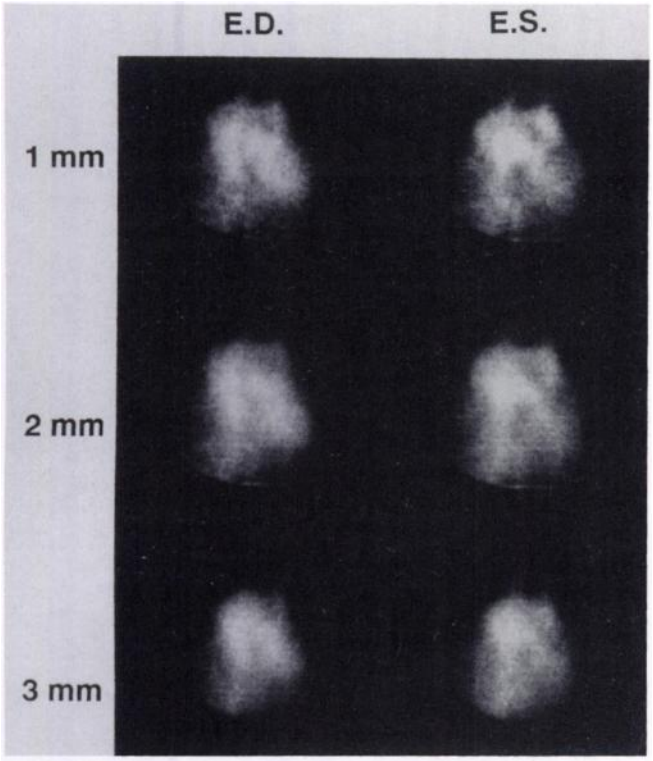

FIGURE 3. End-diastolic and end-systolic images of gated blood-pool scans performed with ^{99m}Tc-HSA using the 3-, 2-, and 1-mm pinhole apertures in the same animal.

risk to the personnel performing the procedure and contamination of blood prior to reinjection is possible. Blood handling can be somewhat decreased with the whole blood in vitro method (*9*). With the in vivo method, poorer quality images are obtained but the labeling procedure is simpler and does not require handling blood. However, the procedure is still relatively complex and requires two injections separated by 20 to 30 min. In addition, as in human subjects, the quality of radiolabeling is dependent

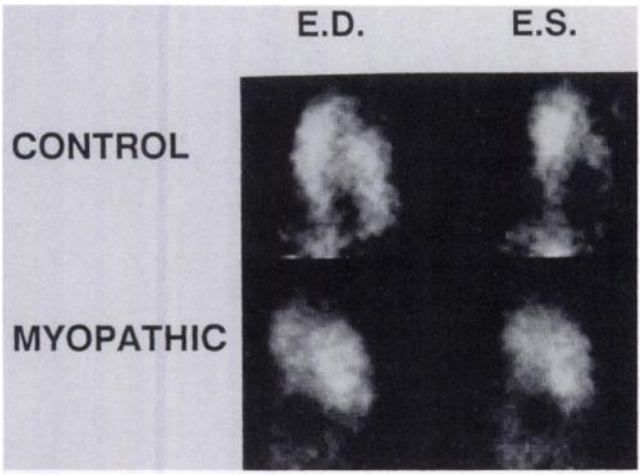

FIGURE 4. End-diastolic and end-systolic gated blood-pool images in 8.5-mo-old Syrian hamsters with cardiomyopathy and age-matched controls.

on clinical condition and drug regimen, the labeling efficiency is not predictable, and there is the possibility of occasional non-labeling (*16,20–21*). The modified in vivo method is a compromise between these methods.

Radiolabeled HSA has the advantages of simplicity of labeling, no contact with blood, and lack of dependence on clinical status. Previously, it has been demonstrated that ^{99m}Tc-HSA is inferior to ^{99m}Tc-labeled RBCs for blood-pool imaging in humans (*8*). In this report, we demonstrate that ^{99m}Tc-IgG and HSA yield adequate images for the evaluation of ventricular function in small animals. With both HSA and IgG, the contrast between liver and blood pool was less than that with radiolabeled RBCs. This could be related to the fact that the regional hematocrit in the liver is lower than in the peripheral circulation (*25*) or that extravascular HSA or IgG was accumulated in the liver. Since proteins radiolabeled with ^{99m}Tc via nicotinyl hydrazine derivatives have been shown to be very stable in vivo (*22*), it was anticipated that HSA labeled by this method would be a superior blood-pool agent compared to HSA labeled by the conventional stannous reduction method. However, the results indicated that the two HSA preparations were equivalent.

The 15-mCi dose used in our studies was significantly higher than doses previously reported in blood-pool imaging in rodents. However, this dose did not result in significant dead-time count losses.

Ejection fractions calculated with ^{99m}Tc-IgG, ^{99m}Tc-HSA (I), and in vitro labeled RBCs were slightly higher than the values obtained with in vivo labeled RBCs as illustrated in Table 2. The relatively lower ejection fraction calculated from in vivo RBCs may be due to a lower labeling efficiency of the red cells resulting in poor quality images that may affect the calculation of ejection fraction.

An additional factor influencing image quality is image resolution. In the case of pinhole collimators, resolution and sensitivity is highly dependent on object-to-collimator distance. The closer the collimator is to the object the better the sensitivity. This becomes particularly important for the small apertures. For this reason, we imaged the animal with the collimator in contact with the body. We were surprised that the theoretical 9-fold difference in sensitivity between the 1- and 3-mm apertures was not observed—rather a 4-fold difference in time was required to record data with the 1-mm pinhole compared to the 3-mm aperture. The reason for this difference was probably due to a small change in distance from aperture to animal when the data were recorded. The resolution of a pinhole collimator is fixed by the aperture's effective diameter (at low energies equal to the physical diameter), while the magnification is set by the object-to-collimator distance. The practical working ranges are bounded by two limbs. The outer limit is set by the intrinsic resolution of the detector (resolution cannot be improved by casting a smaller spot on the crystal than it can intrinsically resolve). The inner limit is arbitrarily defined as the distance at

which two adjacent point sources cast discernible spots that just fill the whole field of the detector. These considerations suggest that for small objects like the <1 cm long hamster heart an acceptable tradeoff of resolution and sensitivity occurs when the 2-mm aperture pinhole is placed on the animal's chest. The efficiency of data collection is important to minimize anesthesia time and consequent risks to the animals under study. From a practical perspective, the total time for setup and data acquisition should be kept to <15 min/animal.

Administered doses of 15 mCi were selected for this trial to maximize the available count rate while limiting the radiation exposure to the investigators. The problems of shielding, handling, and caring for large numbers of radioactive animals precluded the use of higher doses in an open laboratory environment.

Overall, this study suggests that an acceptable combination of radiopharmaceutical and collimator for evaluating cardiac function in small animals is a ^{99m}Tc-labeled protein (IgG or HSA) and a 2-mm pinhole colllimator. The proteins combine the qualities of ease of preparation, good image definition, and precise EF determination. The 2-mm pinhole offers a good compromise between image definition and sensitivity.

REFERENCES

1. Rocco TP, Dilsizian V, Fischman AJ, Strauss HW. Evaluation of ventricular function in patients with coronary artery disease. *J Nucl Med* 1990;30:1149–1165.
2. Dilsizian V, Rocco TP, Bonow RO, Fischman AJ, Boucher CA, Strauss HW. Cardiac blood-pool imaging. II. Applications in noncoronary heart disease. *J Nucl Med* 1990;31:10–22.
3. McIntosh GH, Barden LR, Buttfield IH. Gated blood-pool studies of cardiac function in the rat and marmoset. *J Nucl Med* 1983;24:728–731.
4. Eckelman W, Richards P, Hauser W, Atkins H. Technetium-labeled red blood cells. *J Nucl Med* 1971;12:22–24.
5. Smith TD, Richards P. A simple kit for the preparation of Tc-99m-red blood cells. *J Nucl Med* 1976;17:126–132.
6. Atkins HL, Eckelman WC, Klopper JF, et al. Vascular imaging with ^{99m}Tc-red blood cells. *Radiology* 1973;106:357–360.
7. Pavel DG, Zimmer AM, Patterson VN. In vivo labeling of red blood cells with Tc-99m: a new approach to blood-pool visualization. *J Nucl Med* 1977;18:305–308.
8. Callahan RJ, Froelich JW, McKusick KA, Leppo J, Strauss HW. A modified method for in vivo labeling of red cells with Tc-99m. *J Nucl Med* 1982;23:315–318.
9. Srivastava SC, Babich JB, Richards P. A new kit method for selective labeling of erythrocytes in whole blood with technetium-99m [Abstract]. *J Nucl Med* 1983;24:128P.
10. Benjamin PP. A rapid and efficient method of preparing ^{99m}Tc-human serum albumin: its clinical application. *Int J Appl Radiat Isot* 1969;20:187–194.
11. Eckelman WC, Meinken G, Richards P. Tc-99m-human serum albuminutes. *J Nucl Med* 1971;12:701–710.
12. Millar AM, Hannan WJ, Sapru RP, et al. An evaluation of six kits of Tc-99m-human serum albumin injection for cardiac blood-pool imaging. *Eur J Nucl Med* 1979;4:91–94.
13. Rhodes BA. Considerations in radiolabeling of albuminutes. *Semin Nucl Med* 1974;4:281–293.
14. Thrall JH, Freitas JE, Swanson D, et al. Clinical comparison of cardiac blood pool visualization with Tc-99m-red blood cells labeled in vivo and with Tc-99m-human serum albumin. *J Nucl Med* 1978;19:796–803.
15. Atkins HL, Klopper JF, Ansar AN, et al. A comparison of Tc-99m-labeled human serum albumin and in vitro labeled red cells for blood pool studies. *Clin Nucl Med* 1980;5:166–169.
16. Hegge FN, Hamilton WG, Larson SM, et al. Caridac chamber imaging: a comparison of red blood cells labeled with Tc-99m in vitro and in vivo. *J Nucl Med* 1978;19:129–134.
17. Atkins HL, Srivastava SC, Meiken GE, Richards P. Biological bheavior of erythrocytes labeled in vivo and in vitro with Tc-99m. *J Nucl Med Technol* 1985;13:136–139.
18. Neuman P, Schica H, Schurnbrand P, Bahre M, Henrich D. Visualizing cardiac blood pool: comparison of three labeling methods. *Eur J Nucl Med* 1983;8:463–466.
19. Armstrong LK, Ruel JM, Christian PE, Taylor A. Variation in gated blood-pool image quality using in vivo, modified in vivo, and in vitro red blood cells labeling technique. *J Nucl Med Technol* 1986;14:63–65.
20. Seawright SJ, Maton PJ, Greenall J, et al. Factors affecting in vivo labeling of red blood cells [Abstract]. *J Nucl Med Technol* 1983;11:95.
21. Callahan RJ. Radiolabeled red blood cells as diagnostic radiopharmaceutical. *Radiopharmaceuticals: Progress and Clinical Perspectives.* 1986;2:41–60.
22. Abrams MJ, Juweid M, tenKate CI, et al. Tc-99m-human polyclonal IgG radiolabeled via the hydrazino nicatinamide derivative for imaging focal sites of infection in rats. *J Nucl Med* 1990: in press.
23. Homburger F. Myopathy of hamster dystrophy: history and morphological aspects. *Ann NY Acad Sci* 1979;317:2–17.
24. Kubota K, Som P, Oster ZH, et al. Detection of cardiomyopathy in an animal model using quantitative autoradiography. *J Nucl Med* 1988;29:1697–1703.
25. Klopper JF, Spencer RP, Srivastava SC, et al. Studies of radionuclide determination of regional hematocrit in dogs. *Int J Nucl Med Biol* 1979;6:68–72.